LRP-6 is a coreceptor for multiple fibrogenic signaling pathways in pericytes and myofibroblasts that are inhibited by DKK-1

Shuyu Ren[a,b], Bryce G. Johnson[a,b], Yujiro Kida[a,b], Colin Ip[a,b], Kathryn C. Davidson[c,d], Shuei-Liong Lin[e], Akio Kobayashi[f], Richard A. Lang[g], Anna-Katerina Hadjantonakis[h], Randall T. Moon[c,d], and Jeremy S. Duffield[a,b,d,1]

[a]Division of Nephrology and [b]Center for Lung Biology, Department of Medicine and Pathology, [c]Howard Hughes Medical Institute, and [d]Institute for Stem Cell and Regenerative Medicine, University of Washington, Seattle, WA 98109; [e]Department of Physiology and Medicine, National Taiwan University Hospital, Taipei 100, Taiwan; [f]Renal Division, Department of Medicine, Harvard Medical School, Boston, MA 02115; [g]Cincinnati Children's Hospital Medical Center, Cincinnati, OH 45229; and [h]Developmental Biology Program, Sloan-Kettering Institute, New York, NY 10065

Edited by Michael Karin, University of California, San Diego School of Medicine, La Jolla, CA, and approved December 7, 2012 (received for review June 29, 2012)

Fibrosis of vital organs is a major public health problem with limited therapeutic options. Mesenchymal cells including microvascular mural cells (pericytes) are major progenitors of scar-forming myofibroblasts in kidney and other organs. Here we show pericytes in healthy kidneys have active WNT/β-catenin signaling responses that are markedly up-regulated following kidney injury. Dickkopf-related protein 1 (DKK-1), a ligand for the WNT coreceptors low-density lipoprotein receptor-related proteins 5 and 6 (LRP-5 and LRP-6) and an inhibitor of WNT/β-catenin signaling, effectively inhibits pericyte activation, detachment, and transition to myofibroblasts in vivo in response to kidney injury, resulting in attenuated fibrogenesis, capillary rarefaction, and inflammation. DKK-1 blocks activation and proliferation of established myofibroblasts in vitro and blocks pericyte proliferation to PDGF, pericyte migration, gene activation, and cytoskeletal reorganization to TGF-β or connective tissue growth factor. These effects are largely independent of inhibition of downstream β-catenin signaling. DKK-1 acts predominantly by inhibiting PDGF-, TGF-β–, and connective tissue growth factor-activated MAPK and JNK signaling cascades, acting via LRP-6 with associated WNT ligand. Biochemically, LRP-6 interacts closely with PDGF receptor β and TGF-β receptor 1 at the cell membrane, suggesting that it may have roles in pathways other than WNT/β-catenin. In summary, DKK-1 blocks many of the changes in pericytes required for myofibroblast transition and attenuates established myofibroblast proliferation/activation by mechanisms dependent on LRP-6 and WNT ligands but not the downstream β-catenin pathway.

Fibrosis of the internal organs, resulting from subclinical injury to the organ over a period of time or from acute severe injury or inflammation, is a major global health problem. All organs may be affected by fibrosis, which matures into microscopic or macroscopic scarring within the tissue parenchyma. At present there are few therapies that specifically target the process of fibrogenesis, despite increasing evidence suggesting that fibrogenesis per se provokes further decline in organ function, inflammation, and tissue ischemia (1). In addition, myofibroblasts themselves are inflammatory cells that generate cytokines, chemokines, and radicals that promote injury. Myofibroblasts appear as a result of a transition from pericytes, cells that normally nurse, maintain, and regulate the microvasculature (2, 3). The transition from pericytes to myofibroblasts results in an unstable microvasculature leading to aberrant angiogenesis or rarefaction (3). These microvascular changes ultimately provoke tissue ischemia. Therefore, the myofibroblast and its transition from resident pericyte or fibroblast is a major new target for therapeutics to counter the deleterious consequences of tissue injury.

Recently, SNPs in LRP-6, a transmembrane coreceptor for WNTs that binds to Frizzled (Frz) receptors and thereby to the WNT/β-catenin signaling cascade, have been identified as independent risk factors for cardiovascular diseases. However, the mechanisms still are obscure (4, 5).

The WNT/β-catenin signaling pathway is a major regulator of cell function both in embryonic development and in adults. Both elevated and attenuated levels of signaling that fall outside the normal homeostatic range of WNT signaling are linked to abnormal embryonic development and to diverse disease states (6). Increasing evidence indicates that WNT signaling plays critical roles in tissue regeneration and immune responses to injury and infection (7). However, the signaling cascade and the cellular responses are complex and context specific (8).

Previous studies have highlighted the importance of WNT/β-catenin in kidney regeneration (9), and studies of chronic disease of the kidney glomerulus and liver sinusoids suggest that persistent activation of WNT/β-catenin is deleterious (10), but the role of WNT signaling in myofibroblasts and their precursors, pericytes of the kidney capillaries, was not studied (2). Here we explore the consequences of reactivating WNT/β-catenin signaling in pericytes and myofibroblasts after kidney injury.

Results and Discussion

Wnt/β-Catenin Pathway Is Up-Regulated in Myofibroblasts in Kidney Disease. To explore the extent of the activation of the canonical WNT pathway in cells of the normal kidney, we studied two distinct lines of mice that are transgenic for reporters of WNT/β-catenin signaling. *Axin2*$^{+/lacz}$ generates β-gal in cells expressing the endogenous WNT/β-catenin target gene, Axin2. (Fig. 1*A*) (11). *TCF/LEF-H2B-GFP*^{Tr} is a recently validated transgenic line of mice reporting β-catenin activity by nuclear GFP expression. It exhibits enhanced sensitivity and specificity over previous reporters of β-catenin nuclear activity (Fig. 1*A*) (12). In normal kidneys of *Axin2*$^{+/lacz}$ mice there is extensive WNT/β-catenin signaling in the papilla, and there are more restricted responses in the normal medulla and kidney cortex, as we have demonstrated previously (Fig. S1*A*) (9). Among the cells expressing lacZ were podocytes, vascular smooth muscle of arterioles, and some pericytes (Fig. 1 *B–D* and Fig. S1 *A* and *B*). In response to injury initiated by obstructing urine flow from the kidney (the unilateral ureteric obstruction [UUO] model), there was marked increase in lacZ staining in the scar-forming cells known as "myofibroblasts" that derive from pericytes (Fig. 1 *B–D*). Although collecting duct cells and cells of the loop of Henle showed *Axin2*-

Author contributions: S.R. and J.S.D. designed research; S.R., B.G.J., C.I., S.-L.L., and J.S.D. performed research; Y.K., K.C.D., S.-L.L., A.K., R.A.L., A.-K.H., R.T.M., and J.S.D. contributed new reagents/analytic tools; S.R., B.G.J., C.I., and J.S.D. analyzed data; and K.C.D., R.T.M., and J.S.D. wrote the paper.

Conflict of interest statement: S.R. and J.S.D have submitted patent applications for the use of DKK-1 in fibrosis.

This article is a PNAS Direct Submission.

[1]To whom correspondence should be addressed. E-mail: jeremysd@uw.edu.

This article contains supporting information online at www.pnas.org/lookup/suppl/doi:10.1073/pnas.1211179110/-/DCSupplemental.

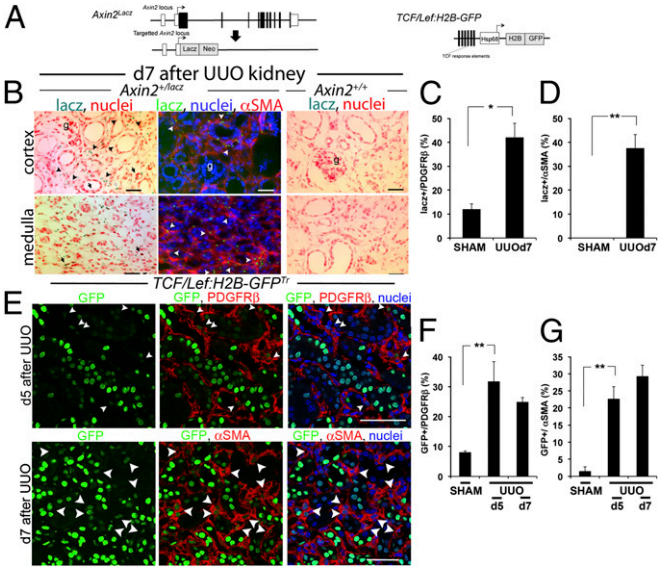

Fig. 1. WNT/β-catenin signaling is activated during kidney injury in the pericyte/myofibroblast cell compartment. (*A*) Schema showing the *Axin2*^{LacZ} allele and the *TCF/Lef:H2B-GFP* transgene, which report WNT/β-catenin signaling. (*B–D*) WNT responses identified by blue stain or green fluorescence in cells (*B*) and quantified in graphs (*C* and *D*) during kidney injury induced by UUO in *Axin2*$^{+/lacz}$ reporter mice are seen predominantly in myofibroblasts (arrowheads), but no stain is seen in Axin2$^{+/+}$ kidneys. (*E–G*) WNT/β-catenin responses identified by nuclear GFP in confocal images (*E*) of kidneys from *TCF/Lef:H2B-GFP*^{Tr} reporter mice after UUO, highlighting PDGFRβ^{+} cells or αSMA cells, two markers for myofibroblasts in diseased kidney, and quantified (*F* and *G*) by PDGFRβ- or αSMA-staining cells expressing nuclear GFP. $*P < 0.05$, $**P < 0.01$. $n = 4$ per group. Error bars indicate SEM.

lacZ staining, little lacZ was detected in distal and proximal tubules in either normal or diseased kidneys (Fig. S1*B*).

To visualize this WNT response in greater detail, we localized WNT reporter activity in *TCF/LEF-H2B-GFP*^{Tr} mice. In normal kidney, β-catenin responses were more extensive than previously appreciated. We have shown previously that in normal kidney, proximal and distal epithelium exhibits little endogenous WNT/β-catenin reporter activity (9). In contrast, in *TCF/LEF-H2B-GFP*^{Tr} mice there was evidence of WNT reporter activity in many of these cells (Fig. 1*E* and Fig. S1 *C–G*). However, like the *Axin2*$^{+/lacz}$ reporter, a minority of pericytes showed active signaling in normal kidney. Following kidney injury, WNT/β-catenin reporter activity increased in epithelial cell compartments, but there was a much greater increase in the pericyte/myofibroblast population of cells (Fig. 1 *E–G* and Fig. S1*C*).

Kidney Myofibroblasts Up-Regulate Wnt Pathway Genes and Wnt Reporter Activity. To explore further the activation of the WNT pathway in kidney myofibroblasts, we purified nonactivated pericytes (normal kidney), activated pericytes (from day 2 after UUO), and myofibroblasts transitioned from pericytes (from days 5, 7, and 10 after UUO) by flow cytometric sorting of single-cell digests from kidneys of the *Coll-GFP*^{Tr} reporter mouse, which specifically expresses GFP in these cells (13). Purified cells showed marked up-regulation of pericyte genes, including P75 NGFR (*Ngfr*) (Fig. S2*A*), and at baseline expressed detectable levels of NG2 (*Cspg4*) and PDGFRβ (*Pdgfrb*) that were modestly up-regulated over time postinjury (Fig. S2*D*, Table S1). We found prototypical profibrotic genes expressed in normal kidney and up-regulated over time postinjury in our disease model, including *Col1a1*, *Tgfb1*, *Ctgf*, and *Fgf2*. We also observed up-regulation of the phosphatonin *Fgf23*, which has been implicated in the pathogenesis of cardiovascular disease (Fig. S2*A*). WNT ligands, including *Wnt2*, *3*, *7b*, *8a*, *8b*, and *10a*, were up-regulated. Pericytes also express cell-surface receptors (Fzd) and coreceptors (Lrp5, Lrp6) for WNT responsiveness (Fig. S2*B*). As the course of kidney disease progressed, there was a modest up-regulation of the Dickkopf-related protein (DKK) family of mRNAs known to inhibit canonical WNT signaling via direct binding to the LRP-5 and LRP-6 coreceptors (Fig. S2*C*). Other WNT downstream target genes, including sFLT1 and WISP1, which play important roles in noncanonical and canonical WNT signaling pathways, respectively, also were up-regulated, consistent with activated WNT/β-catenin and also noncanonical WNT pathways (Fig. S2*C*).

DKK-1 Triggers G1 Cell-Cycle Arrest and Down-Regulates Activation in Myofibroblasts. To test the function of WNT/β-catenin pathway activation in myofibroblasts, we generated primary myofibroblast cultures from *Coll-GFP*^{Tr} mice that had kidney fibrosis (13). Myofibroblasts also expressed WNT ligands and receptors (Fig. S3*A*). DKK-1 has been reported to inhibit the WNT/β-catenin pathway by binding to LRP-5 or LRP-6. We cloned *Dkk1* and expressed soluble DKK-1 or the DKK-1-GFP fusion protein (Fig. S3*B*) in HEK293 cells. Soluble DKK-1-GFP binding to unlabeled cell lines was markedly enhanced by overexpression of LRP-5 or LRP-6 (Fig. S3*C*), and DKK-1-GFP readily bound to the surface of cultured myofibroblasts without the requirement for receptor overexpression (Fig. S3*D*), indicating high receptor density for DKK-1 on myofibroblasts. DKK-1 protein specifically blocked entry of myofibroblasts into the cell cycle induced by serum at the G1 checkpoint (Fig. 2 *A–F* and Fig. S3*E*), resulting in inability to proliferate (Fig. 2*B*).

To understand the mechanisms better, we tested the effect of DKK-1 on the steady-state level of β-catenin protein. Cytosolic and nuclear β-catenin increased 1 h and 16 h after serum activation, an effect decreased by DKK-1 at 16 h (Fig. 2*G*), confirming DKK-1 inhibits WNT/β-catenin signaling but suggesting early DKK-1 responses may occur independent of regulation of β-catenin protein (Fig. 2*G*). Transcripts for αSMA (*Acta2*), a marker of myofibroblast activation, were increased by serum at 24 h, and DKK-1 significantly reduced this activation (Fig. 2*H*), suggesting that DKK-1 may regulate activation also.

Systemic Delivery of DKK-1 Inhibits Myofibroblast Expansion and Fibrosis. Next we tested whether DKK-1 inhibited pericytes and myofibroblasts in vivo. DKK-1 was delivered systemically using an

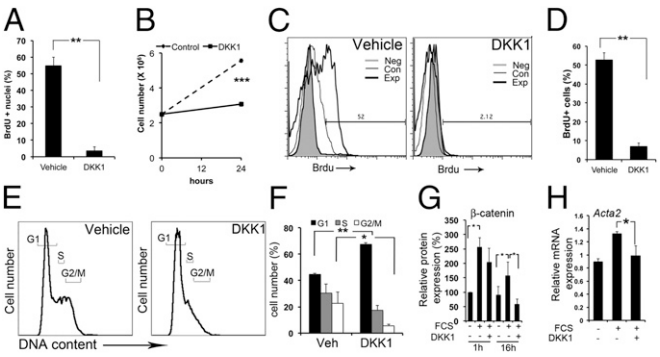

Fig. 2. DKK-1 binds to myofibroblasts and blocks proliferation by G1/S cell-cycle arrest in vitro. (*A*) Graph showing BrdU nuclear incorporation in quiescent myofibroblasts stimulated for 3 h with 3% FCS and DKK-1 or vehicle. (*B*) Coulter-counted kidney quiescent myofibroblasts stimulated for 24 h with 3% FCS and DKK-1 or vehicle. (*C* and *D*) Flow cytometric plots (*C*) and graph (*D*) showing BrdU uptake in myofibroblasts stimulated for 3 h with 3% FCS and DKK-1 or vehicle. (*E* and *F*) Propidium iodide DNA content plots (*E*) and graph (*F*) showing quiescent myofibroblasts stimulated for 24 h with 3% FCS and DKK-1 or vehicle. (*G*) The effect of DKK-1 on cytoplasmic and nuclear β-catenin protein. Serum increases β-catenin, an effect not modulated by DKK-1 at 1 h, but DKK-1 markedly reduces β-catenin levels at later time points. (*H*) qPCR data showing myofibroblast expression of *Acta2* after treatment with FCS or FCS + DKK-1. $*P < 0.05$, $**P < 0.01$, $***P < 0.001$. $n = 4$ per group. Error bars indicate SEM.

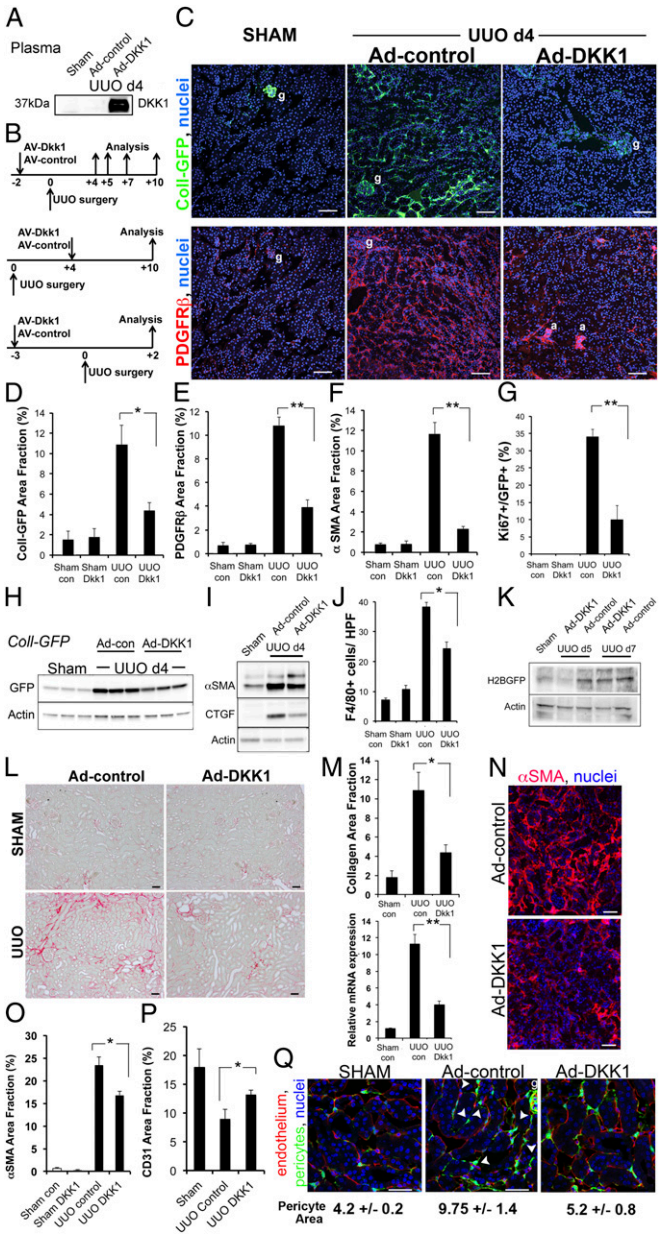

Fig. 3. DKK-1 blocks pericyte activation and transition to myofibroblasts and reverses myofibroblast activation in vivo, inhibiting fibrogenesis, capillary rarefaction, and inflammation. (*A*) Western blots of 5 μL of plasma from mice 5 d after i.v. injection of Ad-control or Ad-DKK-1 and from mice subjected to sham surgery and injected with control. (*B*) Experimental schemata for adenoviral administration, kidney injury, and analysis in the UUO model. (*C–M*) Prevention studies. (*C*) Low-magnification confocal images of kidney cortex 4 d after sham operation or UUO in *Coll-GFP^{Tr}* mice that had received Ad-control or Ad-DKK-1 6 d previously, showing Coll-GFP cells or PDGFRβ cells. g, glomerulus; a, arteriole. (*D–F*) Graphs showing quantification of Coll-GFP cells, PDGFRβ cells, and αSMA cells in kidney 4 d after UUO. (*G*) Proportion of Coll-GFP cells that express the proliferation marker Ki67. (*H* and *I*) Western blot of GFP (*H*) or αSMA/CTGF (*I*) in whole Coll-GFP mouse kidney 4 d after UUO. (*J*) Quantification of macrophage numbers in kidney sections detected by F4/80 staining. (*K*) Western blot quantifying canonical WNT signaling by detecting the H2B-GFP fusion protein after Ad-DKK-1 vs. Ad-control treatment of *TCF/Lef:H2B-GFP^{Tr}* reporter mice during UUO kidney injury. (*L*) Sirius red-stained kidneys 10 d after UUO. (*M*) Morphometry of Sirius red-stained collagen (*Upper*) or qPCR for *Col1a1* transcripts (*Lower*) 10 d after UUO in mice treated with Ad-control vs. Ad-DKK-1. (*N–P*) Reversal studies. Confocal Images (*N*) and morphometric quantification (*O*) of αSMA staining 10 d after UUO in mice treated with Ad-control or Ad-DKK-1 from day 4. (*P*) Quantification of capillary density 10 d after UUO. Note that rarefaction occurs in response to kidney disease, but DKK-1 partially reverses rarefaction. (*Q*) Pericyte detachment. Images and quantification of pericyte area in Coll-GFP mice 2 d after UUO in the presence of circulating DKK-1 or control. Note that injury to the kidney stimulated pericyte spreading and detachment from endothelium (arrowheads). $^*P < 0.05$, $^{**}P < 0.01$. $n = 4–6$ per group. Error bars indicate SEM.

adenoviral delivery system that generates high-level expression of circulating DKK-1 protein (Fig. 3*A*). We tested circulating DKK-1 on both the development and progression of kidney fibrosis using three different experimental designs (Fig. 3*B*). In preventative studies using the UUO model, DKK-1 profoundly inhibited pericyte expansion, proliferation, and transition to myofibroblasts (Fig. 3 *C–I*), resulting in reduced fibrosis (Fig. S4). The inhibition on day 4 after UUO was associated with a marked reduction in inflammation (Fig. 3*J*) and epithelial injury (Fig. S4 *A* and *B*). Moreover, expression of the WNT/β-catenin reporters in kidney myofibroblasts was reduced, particularly at the earlier time points (Fig 3*K*). These studies were extended to day 10 after UUO injury, and there was a substantial reduction in organ fibrosis and collagen transcripts (Fig. 3 *L–M*).

To study this effect in more detail, we performed a reversal study in which DKK-1 was delivered after disease onset, and fibrosis extent was assessed 10 d after UUO (Fig. 3 *N–P*). Myofibroblast accumulation, proliferation, deposition of interstitial fibrosis, and rarefaction of the capillaries were inhibited. Furthermore, as in the preventative studies, DKK-1 inhibited inflammation and epithelial injury (Fig. S4 *A–C*). Because recent evidence indicates that myofibroblasts in kidney arise from pericyte precursors which detach from peritubular capillaries in response to injury (2), we examined the effect of DKK-1 on pericyte precursor detachment, spreading, and migration in *Coll-GFP^{Tr}* reporter mice. DKK-1 inhibited pericyte detachment from capillaries at early time points in this model (Fig. 3*Q*).

We tested whether DKK-1 could inhibit disease in a second model of inflammation and fibrosis, ischemia reperfusion injury (U-IRI) of a single (unilateral) kidney, a recognized model of chronic kidney disease following acute kidney injury (9). We performed a reversal study in this model and characterized the extent of scarring in the kidney 10 d after the initial U-IRI. Circulating DKK-1 inhibited myofibroblast accumulation, inflammation, and interstitial fibrosis and reduced epithelial injury (Fig. S4 *E–K*) sufficiently to reverse existent fibrosis (Fig. S4*L*).

DKK-1 Blocks PDGF-Stimulated Proliferation of Kidney Pericytes by an LRP-6, P42/P44 MAPK-Dependent Mechanism. To study the mechanism of action of DKK-1, we tested its effects on primary kidney pericyte cultures, the precursors of myofibroblasts (2, 13). PDGF and TGF-β signaling in pericytes are important factors in the detachment of pericytes from capillaries and their transition to myofibroblasts (3, 14) and as such are important factors in driving fibrosis. Connective tissue growth factor (CTGF) and its homolog CCN1 (Cyr61) also have been implicated in fibrosis and wound healing (15). Pericytes were stimulated by PDGF-BB to enter the cell cycle (Fig. 4*A*), but other profibrogenic growth factors had no effect. Unexpectedly, exogenous addition of WNT3a did not stimulate proliferation. DKK-1 markedly attenuated PDGF-BB–stimulated proliferation (Fig. 4*B*). PDGF stimulation down-regulated transcripts for the activation markers CTGF, αSMA, and collagen Iα (1), and DKK-1 further down-regulated those transcripts (Fig. 4*C*), suggesting that DKK-1 therefore may enhance certain PDGF-mediated transcriptional events. None of the factors applied to pericytes affected viability (Fig. 4*D*).

In keeping with a link between PDGF signaling and the WNT pathway in pericyte proliferation, PDGF regulates a number of WNT ligands, including up-regulating *Wnt2* and *5a* and down-regulating *Wnt7a*, *10a*, and *16* (Fig. 4*E*). However, inconsistent with such a link, exogenous WNT3a had no stimulatory effect on proliferation (Fig. 4*A*). Because DKK-1 acts via LRP-5 and LRP-6, and because PDGF regulates WNT transcripts (Fig. 4*E*), we expected DKK-1 to block the endogenous WNT/β-catenin

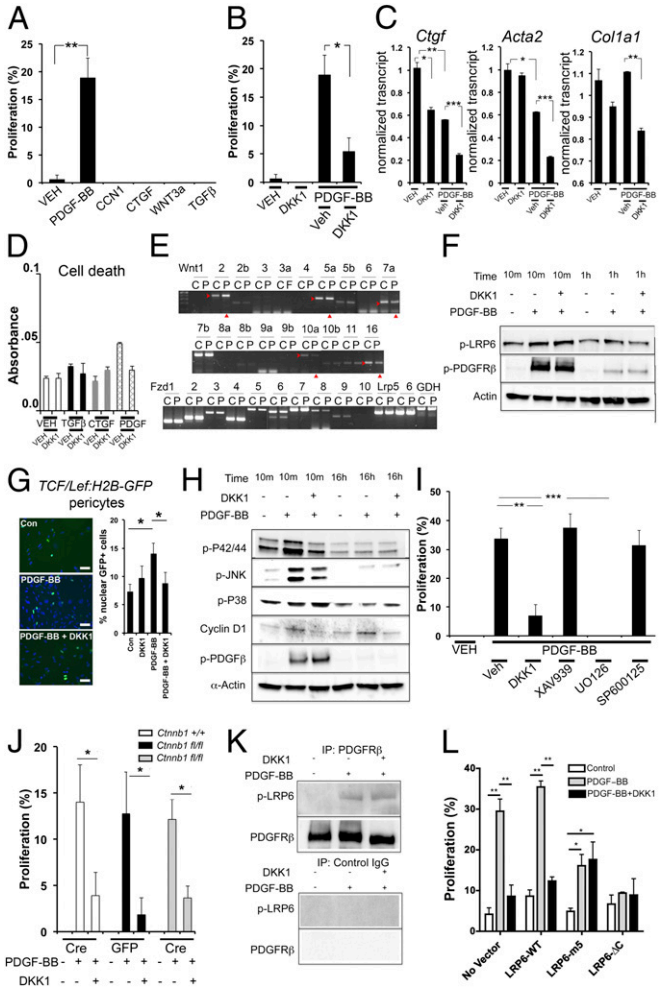

Fig. 4. DKK-1 inhibits PDGF-BB–mediated proliferation of pericytes in vitro by a noncanonical, LRP-6–dependent, P42/44 MAPK-dependent mechanism. (*A*) Graph of BrdU incorporation into quiescent kidney pericytes 6 h after stimulation with cytokines. (*B*) The effect of DKK-1 on PDGF-BB–stimulated proliferation. (*C*) qPCR of genes associated with cell activation in pericytes 48 h after stimulation. (*D*) Quantification of cell viability in pericytes stimulated with cytokines and DKK-1 for 24 h. (*E*) RT-PCR results showing the effect of PDGF-BB on WNT ligands and receptors in pericytes 12 h after stimulation. C, control; P, PDGF; arrowheads indicate regulated genes. (*F*) Western blot time course showing pPDGFRβ and pLRP-6 levels in pericytes. DKK-1 does not affect pLRP-6 at early time points but inhibits pLRP-6 at later time points. (*G*) Fluorescence images and data quantifying nuclear GFP$^+$ (green) in *TCF/Lef:H2B-GFP^{Tr}* canonical WNT reporter pericytes 16 h after PDGF-BB or PDGF-BB + DKK-1. (*H*) Western blot time course of phosphorylated forms of P42/P44, JNK, and P38, PDGFRβ, and total cyclinD1 in pericytes activated by PDGF-BB or PDGF-BB + DKK-1. (*I*) Graph showing the effect of DKK-1 or the canonical WNT inhibitor XAV939, the P42/P44 inhibitor U0126, or the JNK inhibitor SP600125 on PDGF-BB–stimulated BrdU incorporation into quiescent pericytes. (*J*) Graph showing the effect of PDGF-BB on the proliferation of *Ctnnb1$^{fl/fl}$* pericytes that underwent in vitro recombination by expressing Cre recombinase vs. *Ctnnb1$^{fl/fl}$* pericytes that expressed control protein GFP. (*K*) Western blot of pericyte proteins immunoprecipitated by anti-PDGFRβ antibodies or control antibodies detecting pLRP-6 or PDGFRβ. (*L*) Graph showing the effect of expression of LRP-6 (wild type) or dominant-negative forms of LRP-6, LRP-6 with tyrosine-to-methionine mutations at the five tyrosine sites (5m), or LRP-6 lacking the cytoplasmic tail (ΔC) on 3T3 fibroblast proliferation in response to PDGF-BB and DKK-1. $*P < 0.05$, $**P < 0.01$, $***P < 0.01$. $n = 4$–7 per group. All blots are representative of three experiments. (Scale bars, 25 μm.) Error bars indicate SEM.

pathway. Binding of WNT ligands to Fzd receptors and LRP-6 coreceptors leads to activation and phosphorylation of LRP-6 (pLRP-6). Surprisingly therefore, PDGF-BB alone stimulates pLRP-6 (Fig. 4*F*), and DKK-1 initially augments pLRP-6 modestly and inhibits it only at later time points (Fig. 4*F* and Fig. S5 *A*–*C*), indicating that PDGF may coactivate the WNT/β-catenin pathway and that DKK-1 regulates this coactivation. To test this possibility, we assessed whether PDGF-BB regulates the WNT/β-catenin pathway in pericytes cultured from the β-catenin reporter mouse (*TCF/Lef:H2B-GFP^{Tr}*) (Fig. 4*G*). After 16 h with PDGF, nuclear β-catenin activity was increased significantly. This increase was inhibited by DKK-1 (Fig. 4*G*), although the extent of β-catenin activation was much lower than the extent of cells triggered into the cell cycle (Fig. 4*A*), a finding that is consistent with the possibility that DKK-1 inhibits proliferation by a β-catenin–independent pathway.

We therefore explored signaling pathways activated by PDGF-BB but inhibited by DKK-1 (Fig. 4*H* and Fig. S5*D*). PDGF-BB stimulates the P42/P44 MAPK and the JNK signaling pathways. DKK-1 inhibits both these responses. PDGF-BB activates the P38 MAPK pathway, but DKK-1 enhances this response, perhaps explaining why DKK-1 can enhance PDGF-mediated transcription (Fig. 4*C*). As expected, PDGF-BB enhances cyclin D1 expression (Fig. 4*H* and Fig. S5*D*), an effect inhibited by DKK-1. Although WNT3a alone had no apparent impact on cell proliferation (Fig. 4*A*), it nevertheless stimulated the activation of LRP-6 and accumulation of cyclin D1 (Fig. S5*E*), providing evidence that LRP-6 activation by PDGF-BB results in distinct signaling vs. activation by WNT3a.

Because DKK-1 specifically inhibits PDGF-stimulated P42/P44 MAPK and JNK activation (Fig. 4*H*), the relative importance of these pathways was tested using specific inhibitors. The P42/P44 inhibitor U0126 completely replaced DKK-1 function in PDGF-BB–stimulated pericyte proliferation (Fig. 4*I*), whereas the JNK inhibitor SP600125 had no impact. Because there was no apparent linkage between the PDGF-BB–mediated activation of the WNT/β-catenin signaling pathway and its capacity to stimulate proliferation, we tested whether the WNT/β-catenin pathway is necessary for PDGF-mediated proliferation using a small-molecule inhibitor of β-catenin, XAV939 (a Tankyrase inhibitor). Strikingly, XAV939 had no effect (Fig. 4*I*). To confirm this finding, cultured pericytes from kidneys homozygous for the floxed alleles of β-catenin (*Ctnnb1$^{fl/fl}$*) underwent recombination in vitro by transduction with Lenti-Cre virus, and Lenti-GFP virus was used as a control that does not catalyze recombination. One hundred percent of pericytes were transduced by GFP expression, and β-catenin protein was lost 48 h after transduction with Lenti-Cre (Fig. S6). Pericytes lacking β-catenin responded to PDGF and its inhibition by DKK-1 similarly to pericytes with β-catenin (Fig. 4*J*), confirming that PDGF stimulates and DKK-1 inhibits proliferation independently of the canonical WNT pathway, even though LRP-6 is activated. To study whether DKK-1 mediates its effects through an alternative cell-surface signaling mechanism or whether LRP-6 is necessary for the PDGF signaling pathway in this context, we immunoprecipitated PDGFRβ from pericytes and pulled down active pLRP-6 only when the receptor was engaged with ligand (Fig. 4*K*), indicating a close relationship between the two receptors at the time of signaling. Next, we overexpressed dominant-negative mutated forms of LRP-6 in a mouse embryonic fibroblast cell line (3T3) that endogenously expresses PDGFRβ (Fig. 4*L* and Fig. S6). Expression of two different dominant-negative forms of LRP-6, but not the WT form, was sufficient to inhibit proliferation of 3T3 cells in response to PDGF-BB and to prevent DKK-1 effects (Fig. 4*L*), indicating that DKK-1 inhibits proliferation through signaling via LRP-6 and revealing that LRP-6 can be detected in a complex containing PDGFRβ. Finally, because LRP-6 is required for PDGF-induced proliferation, we assessed whether WNT ligands are necessary for PDGF responses by blocking WNT secretion in pericytes using the Porcupine homolog inhibitor, IWP2 (Fig. S7). Porcupine homolog is required for palmitoylation and secretion of all WNTs from cells (16). IWP2, blocked PDGF-stimulated proliferation in a dose-dependent manner without affecting viability, suggesting that WNT engagement of LRP-6 at the cell surface is necessary for PDGF responses in pericytes.

DKK-1 Inhibits TGF-β– and CTGF-Stimulated Activation of Kidney Pericytes via an LRP-6, JNK-Dependent Mechanism. Our in vivo studies showed that DKK-1 prevents pericyte activation, detachment from capillaries, migration, and expression of the myofibroblast marker αSMA (Fig. 3). Previous and current studies (2, 14) suggest that PDGFR signaling does not affect these pericyte changes directly. Therefore we tested the effect of DKK-1 on pericyte activation and migration in response to other cytokines implicated in these processes (17, 18). In contrast to PDGF, TGF-β markedly and rapidly stimulates pericyte migration (Fig. 5 *A*–*C*), and over 48–72 h up-regulates collagen genes and the intermediate filament αSMA (Fig. 5*D*). Similar observations on migration were made by treatment of pericytes with CTGF (Fig. 5 *C* and *D*), an extracellular protein that may signal via β_1-integrins, LRP-1, and possibly LRP-6 (19), and with CCN1 (Fig. S8*A*). TGF-β and CTGF promote marked cytoskeletal reorganization of contractile filaments in pericytes after 24 h of cytokine treatment (Fig. 5*E*). DKK-1 inhibits all migratory, activatory, and cytoskeletal changes in pericytes in response to TGF-β or CTGF (Fig. 5 *A*–*E*) but has no impact on migration in response to CCN1 (Fig. S8*A*). Strikingly, primary cultures of kidney epithelial cells have high endogenous migration that is weakly responsive to these cytokines. DKK-1 has a nonsignificant effect on these cultures (Fig. S3), suggesting DKK-1 has a major effect on pericytes, not epithelium.

We next tested the impact of DKK-1 on activation of LRP-6 in the context of these activating ligands. TGF-β, and CTGF both activate LRP-6 within minutes of cytokine exposure, and, as expected, WNT3a also stimulates LRP-6 activation (Fig. 5*F* and Figs. S5*E* and S8*B*). Within 10 min, DKK-1 weakly activates LRP-6 (Fig. S5*C*) and does not block the activation triggered by TGF-β or WNT3a (Fig. 5*F* and Fig. S8). However, LRP-6 was deactivated by DKK-1 in all activation conditions after 16 h (Fig. S5), indicating LRP-6 is activated rapidly by non-WNT ligands and DKK-1 either augments that signal weakly or does not affect it initially but silences it only at later time points. Because DKK-1 blocks TGF-β–mediated changes to pericytes, we tested whether TGF-β signals via the WNT/β-catenin pathway directly or indirectly. TGF-β regulates WNT ligands in pericytes at 24 h (up-regulating *Wnt2*, *9a*, and *11* and down-regulating *Wnt2b* and *16*) (Fig. 5*G*), but DKK-1 had no impact on these changes. Both TGF-β and CTGF triggered nuclear β-catenin activity in pericytes (Fig. 5*H*); this activity was inhibited by DKK-1, but, as with PDGF, the effect occurred in a minority of cells, suggesting that TGF-β and CTGF may regulate pericyte activation via a WNT/β-catenin–independent pathway and that DKK-1 may inhibit pericyte activation via that same pathway.

We tested the effect of DKK-1 on TGF-β– and CTGF-mediated signaling. Both TGF-β and CTGF stimulate the P42/P44, P38, and JNK pathways. DKK-1 blocks activation of the P42/44 and JNK pathways and augments activation of the P38 pathway (Fig. 5 *I* and *J*). As expected, FAK is activated by both TGF-β and CTGF and is inhibited by DKK-1 (Fig. 5 *I* and *J*). To test whether components of these DKK-1–regulated signaling cascades are responsible for the impact on migration, we measured the effect of DKK-1 on TGF-β activation of the canonical SMAD activation pathway (Fig. S8*C*), which was not affected. Next we used small-molecule inhibitors of activation of TGFβR1 (SB431542), JNK (SP600125), P42/P44 (U0126), or β-catenin (XAV939) in TGF-β– or CTGF-stimulated migration assays. P42/P44, TGFβR1, and β-catenin inhibitors had no significant effect on TGF-β–stimulated migration, but JNK inhibitors blocked migration to TGF-β completely (Fig. 5*K* and Fig. S8*D*), suggesting DKK-1–mediated silencing of JNK signaling is central to its ability to block TGF-β–stimulated migration. Inhibition of CTGF-mediated migration was independent of TGFβR1 activation, was partially dependent on β-catenin and P42/P44 activation, and was most dependent on JNK activation (Fig. 5*L*), highlighting similarities to and differences from TGF-β–mediated migration. CCN1-mediated migration occurred independently of P42/44 and JNK pathways (Fig. S8*A*). Because XAV939 showed little effect on TGF-β–mediated migration, we generated pericytes lacking β-catenin as described above (Fig. 4*J*). Compared

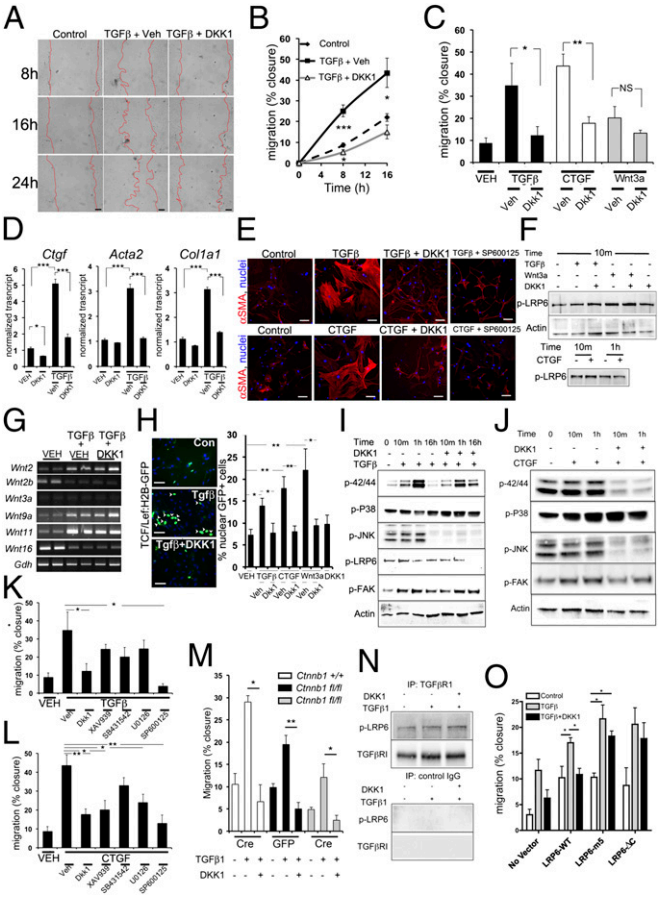

Fig. 5. DKK-1 blocks TGF-β– and CTGF-mediated migration of pericytes in vitro predominantly by a noncanonical, LRP-6–dependent, JNK-dependent mechanism. (*A* and *B*) Images (*A*) and time course graph (*B*) showing migration of kidney pericytes induced by TGF-β and blocked by DKK-1. (Scale bars, 50 μm.) (*C*) Graph of migration at 16 h by pericytes stimulated by TGF-β, CTGF, or WNT3a. All are blocked by DKK-1. (*D*) qPCR of genes associated with cell activation in pericytes. (*E*) Fluorescence images of αSMA showing the cytoskeleton of primary pericytes in control or stimulated conditions for 24 h. (Scale bars, 25 μm.) (*F*) Western blots showing phosphorylated LRP-6 levels in pericytes 10 min after activation with TGF-β or WNT3a in the presence of vehicle or DKK-1 (*Upper*), and after activation with CTGF (*Lower*) (*G*) Thirty-cycle RT-PCR showing the effect of TGF-β or TGF-β + DKK-1 on WNT ligand expression at 8 h. (*H*) Fluorescence images and data quantifying nuclear GFP$^+$ (green) in *TCF/Lef:H2B-GFP^{Tr}* βcatenin reporter pericytes 16 h after stimulation with cytokines +/– DKK-1. (*I*) Western blot time course of phosphorylated forms of P42/P44, JNK, P38, LRP-6, and FAK in pericytes activated by TGF-β or TGF-β + DKK-1. (*J*) Western blots of phosphorylated forms of P42/P44, JNK, P38, and FAK in pericytes activated by CTGF or CTGF + DKK-1. (*K* and *L*) Graphs showing the effect of DKK-1, the canonical WNT inhibitor XAV939, the TGFβR1 kinase inhibitor SB431542, the P42/P44 inhibitor U0126, or the JNK inhibitor SP600125 on TGF-β–stimulated (*K*) or CTGF-stimulated (*L*) migration in quiescent pericytes. (*M*) Graph showing the effect of TGF-β on the migration of *Ctnnb1$^{fl/fl}$* pericytes expressing Cre recombinase vs. *Ctnnb1$^{fl/fl}$* pericytes expressing control protein GFP. (*N*) Western blots of pericyte proteins immunoprecipitated by anti-TGFβR1 antibodies or control antibodies detecting pLRP-6 or TGFβR1. (*O*) Graph showing the effect of expression of LRP-6 (wild type) or dominant-negative forms of LRP-6, 5m, or ΔC on 3T3 fibroblast migration in response to TGF-β and DKK-1. *$P < 0.05$, **$P < 0.01$, ***$P < 0.01$. Error bars indicate SEM. Experiments are from $n = 4$–7 per group. All blots are representative of three experiments.

with controls, in the absence of β-catenin, DKK-1 completely blocked TGF-β–stimulated migration (Fig. 5*M*). However, overall (nonstimulated) migration was reduced in the absence of β-catenin, indicating that DKK-1 can function independently of WNT/β-catenin signaling but that the Wnt/β-catenin pathway

plays a role in the underlying tendency to migrate. To test whether LRP-6 also associated with the TGFβR complex, TGFβR1 was immunoprecipitated, and pLRP-6 was coprecipitated in resting cells. This association increased upon active signaling (Fig. 5*N*). To determine the role of LRP-6 in TGF-β–stimulated migration, we studied expression of the dominant-negative LRP-6 mutants in fibroblasts, as described above (Fig. 4*L*). Strikingly, although TGF-β–mediated migration occurred in the presence of mutant LRP-6, DKK-1 was now ineffective (Fig. 5*O*). Therefore, DKK-1 inhibits TGF-β migration by an LRP-6–dependent mechanism, and active LRP-6 can be detected in a signaling complex with TGFβR1. That TGF-β stimulates migration in the presence of dominant-negative LRP-6 but DKK-1 no longer functions suggests that the endogenous LRP-6 still may be able to interact with TGF-β, whereas DKK-1 binds equally to the mutant forms; further studies will be required to understand LRP-6 interactions with TGFβR1. Finally, to test the role of WNTs in TGF-β–mediated migration and in DKK-1 inhibition, we blocked WNT secretion using IWP2 as described above (Fig. S7). In this setting TGF-β–stimulated migration was blocked completely, suggesting WNT engagement of LRP-6 at the cell surface is necessary for TGF-β response in pericytes.

These studies identify LRP-6 and signaling pathways downstream of LRP-6 as therapeutic targets to intervene in fibrogenesis of the kidney. In addition, they identify the soluble protein DKK-1 and its receptor LRP-6 as important cofactors in multiple signaling pathways activated by TGF-β, CTGF, and PDGF (Fig. S8*E*). Because these multiple pathways are known to contribute to the development of fibrosis and its longer-term consequences on organ function, therapeutically delivered DKK-1 or therapeutic targeting of the LRP-6 receptor are attractive strategies for treating fibrosis, microvascular inflammation, tubule injury, and microvascular rarefaction. Recent studies indicate that mesenchyme-derived cells, either pericytes or resident fibroblasts, are present in all organs and tissues and are the primary source of scar-forming myofibroblasts in multiple tissues (2, 20). Therefore it is likely that the DKK-1/LRP-6 signaling pathway regulates fibrogenesis in multiple organs and tissues.

The MAPK signaling pathways from TGFβR signaling, CTGF signaling, and PDGFR signaling appear to be functionally critical in the mesenchyme-derived perivascular cells in kidney. These pathways have received relatively little attention, and earlier studies have assumed that the canonical pathways activated by these receptors have been dominant in the process of fibrogenesis (14, 21); further studies should focus on these pathways in pericytes and fibroblasts. Our studies show that LRP-6 (and potentially LRP-5), when bound by WNT ligands, interacts physically with PDGFRβ and TGFβR1 upon cognate ligand interaction (Fig. S8*E*). It is possible, therefore, that LRP-6 is responsible for transducing the signal that activates the MAPK pathways. Further studies should address this question. The fact that LRP-6 can function as a coreceptor for multiple pathways raises the question whether it requires an extracellular ligand, distinct from WNT ligands, to effect this interaction. It is likely that soluble ligands such as TGF-β and PDGF are presented at the cell surface bound to extracellular modulators and that these complexes may bind to and be responsible for the recruitment of LRP-6. The studies also indicate that in pericytes and myofibroblasts CTGF activates cells independently of TGF-β, whereas previous reports have suggested CTGF augments TGF-β responses in fibrogenesis. These studies suggest CTGF has a distinct receptor on pericytes and myofibroblasts that has not been fully appreciated. Further studies should define the CTGF receptor in these cells and the interaction of LRP-6 with that receptor.

Genetic studies of LRP-6 and LRP-5 function in mice point to their major role in WNT pathway signal transduction in early and later embryogenesis (5). However, the initial studies suggested that LRP-5/LRP-6 mutations interfered with other signaling pathways, including FGFR1 and Notch Delta (22). Recently, LRP-6 mutations have been found not only in humans with reduced bone mineral density but also in patients with premature cardiovascular disease (4, 5). These reports also have suggested a potential link between LRP-6 and PDGFR signaling. In the context of our current findings, these studies suggest that LRP-6 may regulate multiple signaling pathways in mesenchyme-derived cells that play critical roles in bone mineralization, arterial wall functions, and microvascular wall functions.

We conclude that DKK-1 is antifibrotic and anti-inflammatory by inhibiting multiple signaling pathways in pericytes and myofibroblasts through binding to the cell-surface receptors LRP-5/-6, which in turn act as coreceptors for multiple signaling pathways.

Materials and Methods

Mouse Models. *Col1a1-GFP^{Tr}* (*Coll-GFP*), *Axin2$^{+/lacz}$*, and *TCF/Lef:H2B-GFP^{Tr}* mice were generated and maintained, and genotyping was performed as described (11, 12). *Ctnn1$^{fl/fl}$* mice were obtained from Jackson Labs. All studies were conducted in accordance with protocols approved by the Institutional Animal Care and Use Committee at the University of Washington.

Statistical Analysis. Performed using GraphPad Prism (GraphPad Software). Significance was evaluated by one-way ANOVA.

ACKNOWLEDGMENTS. We thank Dr. Xi He, Dr. Roel Goldschmeding, Dr. William B. Stallcup, and Dr. Gustave Matute-Bello for advice, discussions, and sharing reagents. These studies were funded by National Institutes of Health Grants DK84077 and DK87389 (to J.S.D.), by the University of Washington, and by the University of Washington Institute for Stem Cell and Regenerative Medicine. A.K. was supported by the March of Dimes.

1. Lupher ML, Jr., Gallatin WM (2006) Regulation of fibrosis by the immune system. *Adv Immunol* 89:245–288.
2. Humphreys BD, et al. (2010) Fate tracing reveals the pericyte and not epithelial origin of myofibroblasts in kidney fibrosis. *Am J Pathol* 176(1):85–97.
3. Lin SL, et al. (2011) Targeting endothelium-pericyte cross talk by inhibiting VEGF receptor signaling attenuates kidney microvascular rarefaction and fibrosis. *Am J Pathol* 178(2):911–923.
4. Keramati AR, et al. (2011) Wild-type LRP6 inhibits, whereas atherosclerosis-linked LRP6R611C increases PDGF-dependent vascular smooth muscle cell proliferation. *Proc Natl Acad Sci USA* 108(5):1914–1918.
5. Tamai K, et al. (2000) LDL-receptor-related proteins in Wnt signal transduction. *Nature* 407(6803):530–535.
6. Clevers H, Nusse R (2012) Wnt/β-catenin signaling and disease. *Cell* 149(6):1192–1205.
7. Poss KD (2010) Advances in understanding tissue regenerative capacity and mechanisms in animals. *Nat Rev Genet* 11(10):710–722.
8. Rodilla V, et al. (2009) Jagged1 is the pathological link between Wnt and Notch pathways in colorectal cancer. *Proc Natl Acad Sci USA* 106(15):6315–6320.
9. Lin SL, et al. (2010) Macrophage Wnt7b is critical for kidney repair and regeneration. *Proc Natl Acad Sci USA* 107(9):4194–4199.
10. Cheng JH, et al. (2008) Wnt antagonism inhibits hepatic stellate cell activation and liver fibrosis. *Am J Physiol Gastrointest Liver Physiol* 294(1):G39–G49.
11. Yu HM, et al. (2005) The role of Axin2 in calvarial morphogenesis and craniosynostosis. *Development* 132(8):1995–2005.
12. Ferrer-Vaquer A, et al. (2010) A sensitive and bright single-cell resolution live imaging reporter of Wnt/ß-catenin signaling in the mouse. *BMC Dev Biol* 10:121.
13. Lin SL, Kisseleva T, Brenner DA, Duffield JS (2008) Pericytes and perivascular fibroblasts are the primary source of collagen-producing cells in obstructive fibrosis of the kidney. *Am J Pathol* 173(6):1617–1627.
14. Chen YT, et al. (2011) PDGF receptor signaling activates pericyte-myofibroblast transition in obstructive and post-ischemic kidney fibrosis. *Kidney Int* 80:1170–1181.
15. Wang S, Denichilo M, Brubaker C, Hirschberg R (2001) Connective tissue growth factor in tubulointerstitial injury of diabetic nephropathy. *Kidney Int* 60(1):96–105.
16. ten Berge D, et al. (2011) Embryonic stem cells require Wnt proteins to prevent differentiation to epiblast stem cells. *Nat Cell Biol* 13(9):1070–1075.
17. Sieczkiewicz GJ, Herman IM (2003) TGF-beta 1 signaling controls retinal pericyte contractile protein expression. *Microvasc Res* 66(3):190–196.
18. Hall-Glenn F, et al. (2012) CCN2/CTGF is essential for pericyte adhesion and endothelial basement membrane formation during angiogenesis. *PLoS ONE* 7:e30562.
19. Kawata K, et al. (2012) Role of low-density lipoprotein receptor related protein 1 (LRP1) in CCN2 protein transport in chondrocytes. *J Cell Sci* 125:2965–2972.
20. Walker N, et al. (2011) Resident tissue-specific mesenchymal progenitor cells contribute to fibrogenesis in human lung allografts. *Am J Pathol* 178(6):2461–2469.
21. Leask A (2008) Targeting the TGFbeta, endothelin-1 and CCN2 axis to combat fibrosis in scleroderma. *Cell Signal* 20(8):1409–1414.
22. Kokubu C, et al. (2004) Skeletal defects in ringelschwanz mutant mice reveal that Lrp6 is required for proper somitogenesis and osteogenesis. *Development* 131(21):5469–5480.